Acoustic transient generation by laser-produced cavitation bubbles near solid boundaries

A. Vogel and W. Lauterborn
Drittes Physikalisches Institut, Universität Göttingen, Bürgerstraße 42-44, D-3400 Göttingen, Federal Republic of Germany

(Received 30 October 1987; accepted for publication 30 March 1988)

The acoustic transients emitted after breakdown and cavitation bubble collapse upon focusing a Q-switch laser pulse into a liquid are investigated with special emphasis on their modifications induced by a solid boundary. For measuring the form $p(t)/p_{max}$ of the pressure pulses an optical technique with a resolution of 10 ns has been developed. When $p(t)/p_{max}$ is known, the pressure amplitude can be determined even when a transducer with a rise time much longer than the pulse duration is used. The duration of the transients (20–30 ns) and their pressure are nearly the same after breakdown and spherical bubble collapse. During spherical collapse, a maximum pressure of about 60 kbar is developed inside a bubble with $R_{max} = 3.5$ mm, and on average 73% of the bubble energy loss is transformed into acoustic energy. The sound emission near a solid boundary strongly depends on the normalized distance γ between the bubble and the boundary. The highest pressures at the boundary are achieved for $\gamma \to 0$; for $\gamma = 0.2$ and $R_{max} = 3.5$ mm it has been found that $p = 2.5$ kbar. These results are discussed with respect to the mechanisms of cavitation erosion important for hydraulic cavitation, laser lithotripsy, and ocular surgery.

PACS numbers: 43.25.Yw, 43.30.Nb

INTRODUCTION

It is well known that, when the light from a Q-switched laser is focused into a liquid, an optical breakdown may occur that leads to plasma formation, emission of an acoustic transient, and generation of a cavitation bubble.[1–5] The cavitation bubble is produced by the expanding plasma. Thereby, work is done against the outer pressure in the liquid, and kinetic energy is transformed into potential energy stored in the expanded bubble. The bubble implodes as a result of the outer (static) pressure and a second acoustic transient is emitted upon collapse.[6–15] When the bubble collapses in the vicinity of a solid boundary, a high-speed liquid jet directed toward the wall is produced,[16] and the strength of the acoustic transient is reduced. The jet formation, as well as the emission of the acoustic pulse, depends on the dimensionless distance γ between cavitation bubble and wall,[17–19] with

$$\gamma = s/R_{max}, \tag{1}$$

where R_{max} is the maximum bubble radius and s denotes the distance between the location of the bubble formation and the wall.

The interest in cavitation bubble dynamics mainly arose from their destructive action on solid surfaces in hydraulic machinery which is attributed to the impingement of the jets and to the effect of the acoustic transients. Laser-produced cavitation bubbles offer excellent possibilities for studying these aspects of bubble dynamics in model experiments because they can be made highly spherical and are free from mechanical distortions.[20,21,15] Recently, laser-produced cavitation bubbles have also become important in the medical fields of ophthalmology and urology. In ocular surgery by photodisruption[22–24] and in laser-induced lithotripsy,[25–27] laser pulses are used to produce an optical breakdown with subsequent bubble formation. The surgical effect is related to the mechanism of cavitation erosion because it is probably due to the combined effects of the plasma, the bubble dynamics, and the acoustic transients emitted during breakdown and bubble collapse.[28,29]

It is known from earlier experimental and theoretical work on the sound emission upon spherical cavitation bubble collapse that the pressure pulses have a duration between 10 and 40 ns,[9–11] which is much shorter than the rise time of the fastest pressure transducers commercially available (ca. 150–300 ns). Similar values have been reported for the duration of the acoustic transients caused by the optical breakdown.[3,11,29–31] Exposing these transducers to the acoustic transients to be measured, one records merely the impulse response of the transducer, and the indicated pressure values are lower than the actual ones. Self-made transducers with a rise time of a few nanoseconds are, on the other hand, very insensitive and have to be placed close to the center of the spherical pressure waves. They are not well suited for measuring the sound emission during spherical cavitation bubble collapse because every boundary in the vicinity of the bubble distorts its dynamics. We have, therefore, developed a technique to determine the pressure of short acoustic pulses by using a sensitive pressure transducer with a frequency bandwidth smaller than that of the acoustic pulse. For this, we combined the recording of the acoustical signal with a synchronously performed fast optical measurement of the temporal profile of the pressure pulse. From these data, the actual pressure value can be calculated if the transfer function of the transducer is known.[28] The technique was used to investigate the sound emission caused by the optical break-

 0001-4966/88/080719-13$00.80

down and the bubble collapse and its modification through a solid boundary in the vicinity of the bubble, the latter being especially important for understanding the mechanism of cavitation erosion.

I. MEASUREMENT OF VERY SHORT PRESSURE PULSES

For calculating the actual values of short pressure pulses from the output signal and the transfer function of the pressure transducer, the temporal profile of the pressure pulse has to be known. It was shown by theoretical considerations[9,32] and confirmed by our own measurements that the profile $p(t)$ of the acoustic transients from laser-produced cavitation bubbles can be described by an exponential pulse:

$$p(t) = p_m e^{-(\ln 2/\tau)} H(t), \tag{2}$$

with

$$H(t) = \begin{cases} 1, & \text{for } t \geqslant 0, \\ 0, & \text{otherwise.} \end{cases}$$

Here, p_m is the peak pressure of the pulse and τ is its duration at half-maximum. The Heaviside step function $H(t)$ models the shock front that, due to the high initial pressure values, develops during the first 50 ns after the optical breakdown and the bubble collapse, respectively.[11,33]

Application of the Fourier transform

$$F(\nu) = \int_{-\infty}^{+\infty} f(t) e^{-i2\pi t\nu}\, dt$$

yields the frequency spectrum of the pressure pulse:

$$P(\nu) = \frac{p_m \tau}{\ln 2} \frac{1 - i(2\pi\tau/\ln 2)\nu}{1 + [(2\pi\tau/\ln 2)\nu]^2}. \tag{3}$$

When the pulse duration is much shorter than the rise time of the pressure transducer, the spectral amplitudes of (3) are nearly constant within the bandwidth of the transducer. Therefore, the spectrum of the output signal can be approximated by

$$P_{\text{out}}(\nu) = P(\nu) \cdot T(\nu) \approx (p_m \tau/\ln 2) T(\nu), \tag{4}$$

with $T(\nu)$ representing the transfer function of the transducer. In the following, we assume that the transfer function is constant up to a certain cutoff frequency ν_c and zero for higher frequencies. This approximation is nearly true for the pressure transducer, which was used in the work reported in this article. The cutoff frequency is linked to the rise time t_A of the transducer by

$$\nu_c = 1/2t_A \tag{5}$$

and is most conveniently determined by measuring t_A when the transducer is hit by a laser-induced acoustic transient with duration $\tau \ll t_A$. In a causal linear system, the imaginary part of the transfer function is described by the Hilbert transform of its real part.[34] With the above assumption, this leads to the expression

$$T(\nu) = \left\{ \frac{1}{2} \operatorname{rect}\left(\frac{\nu}{2\nu_c}\right) + i\left[\left(-\frac{1}{\pi\nu}\right) * \frac{1}{2} \operatorname{rect}\left(\frac{\nu}{2\nu_c}\right)\right] \right\} e^{-i2\pi t_0 \nu} \tag{6}$$

for the transfer function of the present transducer, where rect stands for the rectangle function

$$\operatorname{rect}\left(\frac{\nu}{2\nu_c}\right) = \begin{cases} 1, & \text{for } |\nu/2\nu_c| \leqslant \frac{1}{2}, \\ 0, & \text{otherwise,} \end{cases}$$

and * denotes a convolution. The linear phase factor at the end of (6) represents the transit time t_0 of the signal passing the transducer.

The output signal is obtained by combining (4) and (6) and calculating the Fourier transform:

$$p_{\text{out}}(t) = (p_m \tau/t_A \ln 2) \operatorname{sinc}[(t - t_0)/t_A] H(t - t_0), \tag{7}$$

with

$$\operatorname{sinc}[(t - t_0)/t_A] = \sin[\pi(t - t_0)/t_A]/[\pi(t - t_0)/t_A].$$

Comparison of (7) with (2) shows that the peak pressure of an exponential pressure pulse is indicated too low by a factor of

$$m = \tau/t_A \ln 2 \tag{8}$$

when the pulse duration τ is much shorter than the rise time t_A of the pressure transducer. On the other hand, if τ and t_A are known, (8) enables a correction of the indicated pressure values. The factor m expresses how much the sensitivity of the transducer is decreased compared to its nominal sensitivity due to the fact that the length of the pressure pulse is shorter than the thickness of the sensitive layer of the acoustic probe.

II. OPTICAL DETECTION OF ACOUSTIC TRANSIENTS

The scheme for the optical detection of the temporal profile of acoustic transients from laser produced cavitation bubbles is shown in Fig. 1. Similar arrangements have already been used by other workers.[30,35–37] The cavitation bubbles are produced by focusing pulses from a Q-switched laser into a cuvette with water. The probe laser beam from a cw laser is expanded and collimated and illuminates the circular aperture 1, the diameter of which is adjusted so that only the

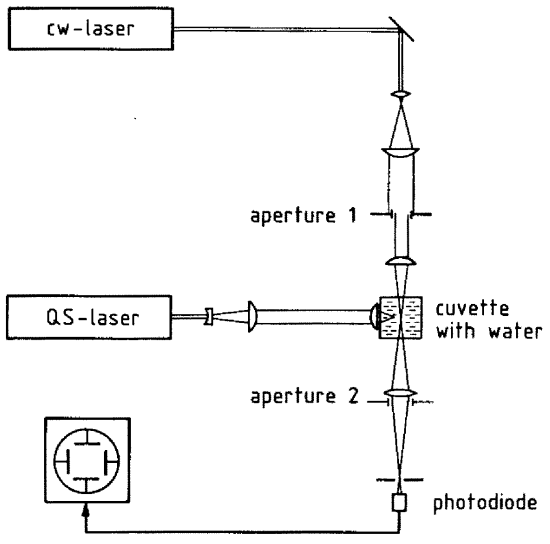

FIG. 1. Scheme for the optical detection of acoustic transients from laser-produced cavitation bubbles.

central part of the beam with nearly homogeneous intensity distribution can pass. This part is focused into the cuvette and the focus is imaged onto the sensitive area of a fast photodiode. The probe beam thereby passes a second circular aperture that has the same diameter as the laser beam. The probe beam waist in the cuvette is located close to the emission center of the acoustic transients that is given by the focus of the beam from the Q-switched laser. When an acoustic pulse passes the probe beam waist, a transient angular deflection ϕ of the probe is produced due to the refractive index change caused by the pressure pulse. As a result, the probe beam is partly blocked out by aperture 2 and the intensity of light arriving at the photodiode is modulated.

The refractive index $n(\mathbf{r},t)$ at the probe beam focus can be separated into the normal refractive index n_0 of the liquid and the refractive index change $n_p(\mathbf{r},t)$ caused by the pressure pulses. Up to a pressure of 2 kbar, $n_p(\mathbf{r},t)$ is approximately proportional to the pressure rise; for higher pressure values, it increases less than proportionally.[38] In the linear domain, the deflection $\phi(\mathbf{r},t)$ of the laser beam is given by[36]:

$$\phi(\mathbf{r},t) \approx \frac{l}{n_0}\frac{\partial n_p(\mathbf{r},t)}{\partial \mathbf{r}} \propto \frac{\partial p(\mathbf{r},t)}{\partial t} \tag{9}$$

provided that the probe beam focus is small compared with the dimension of the acoustic transient; l is the interaction length of the laser beam with the pressure pulse. Because of the spherical geometry of the acoustic transients, (9) is only an approximation. The exact relationship between $\phi(\mathbf{r},t)$ and $p(\mathbf{r},t)$ can only be found by numerical ray tracing.[35]

The voltage signal U from the photodiode depends on the area of overlap between aperture 2 and the probe beam cross section. When the intensity distribution within the probe beam is homogeneous, the relation

$$U(\phi) = \begin{cases} (2U_0/\pi)\left[\cos^{-1}(|\phi|/2\phi_0) - (|\phi|/2\phi_0)\sqrt{1-(|\phi|/2\phi_0)^2}\right], & \text{for } |\phi| \leqslant 2\phi_0, \\ 0, & \text{otherwise} \end{cases} \tag{10}$$

holds, where U_0 is the photodiode voltage for $\phi = 0$ and $2\phi_0$ is the angle of deflection for which the probe beam is just completely blocked out by the aperture. The deflection of the probe beam leads to a reduction of the photodiode voltage independent of its direction so that the voltage is a function of the modulus of the deflection. As shown in Fig. 2, the relationship $U(\phi)$ is nearly linear in a wide range of $|\phi|$. The measurement range and, consequently, the range of linearity can be set by varying the f number of aperture 1 and 2. The range of linearity is much larger than in the arrangements described by Davidson *et al.*,[35] Sullivan *et al.*,[36] and Sigrist.[37] Figure 2 also shows the relationship between U and ϕ for the experimental apparatus described in the next paragraph.

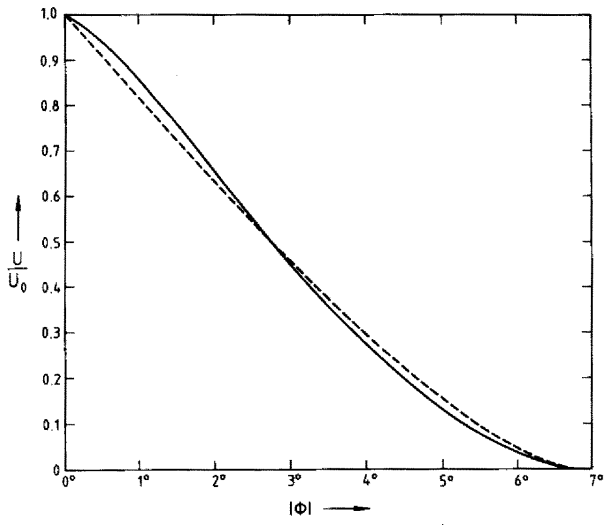

FIG. 2. The normalized photodiode signal U/U_0 as a function of the angular probe beam deflection ϕ: ---, theoretical curve for homogeneous intensity distribution across the probe beam; —, curve determined experimentally for the apparatus described in Sec. III.

The deviations from the theoretical curve are due to the Gaussian intensity profile of the probe beam.

In the approximately linear range of (10), one obtains from (9) and (10) for the change of the photodiode voltage caused by the pressure pulse

$$U_0 - U(t) \propto \left|\frac{\partial_p(\mathbf{r},t)}{\partial t}\right| . \tag{11}$$

Thus the experimental probe beam deflection signal is proportional to the modulus of the time derivative of the pressure pulse at the probe beam position in the liquid.

III. THE EXPERIMENTAL ARRANGEMENT

The experimental arrangement for investigating the acoustic transients from laser-produced cavitation bubbles synchronously by optical and acoustical measurements is shown in Fig. 3. The bubbles are generated in the cuvette filled with distilled water by using a passively Q-switched ruby laser which delivers pulses with an energy of up to 1 J. The focusing lens has a focal length of 25 mm and the cone angle of the focused laser beam is 19.5° (in water). The large cone angle was chosen in order to reduce the probability of multiple optical breakdowns by limiting the volume with suprathreshold light intensity. The transversal mode structure of the ruby laser is irregular, with many high-order modes. The pulse energy is measured with a Hadron 102C energy/power meter. The attenuation factor of the optics delivering the laser pulse into the cuvette was determined in preliminary experiments. For investigating the bubble collapse near a solid boundary, a brass block is placed close to the ruby laser focus. Some acoustic measurements have also been performed with a TEM_{00} Q-switched Nd:YAG laser with a pulse energy of up to 15 mJ. In this case, the cone angle was 16° in air, i.e., about 12° in water.

For the optical detection of the acoustic transients, we

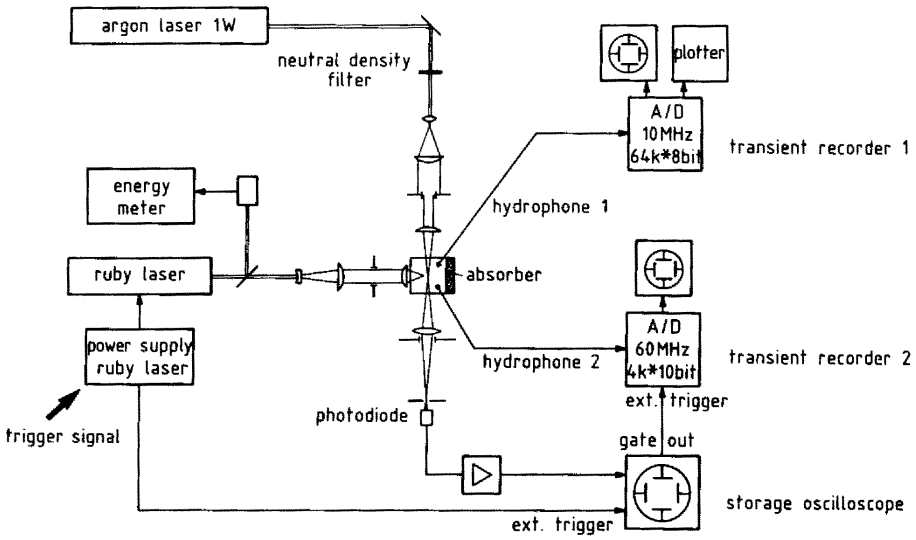

FIG. 3. Experimental arrangement for the investigation of acoustic transient emission during optical breakdown and cavitation bubble collapse.

employed an argon laser. In order to reduce the effect of mode beats between the longitudinal resonator modes, the laser is operated at an output power of 1 W. Thus the interference of a large number of independently oscillating modes produces a light output with little modulation within the frequency bandwidth registered by the photodiode. After attenuation with a neutral density filter, the probe beam is spatially filtered, expanded, collimated, and focused into the cuvette. The focusing optics has an f number of 8.4 (in water). The theoretical diameter of the focal spot is 7.2 μm for a diffraction limited system, but experimentally we determined a spot size of 15 μm. The deviation from the theoretical value is mainly due to the spherical aberrations introduced by the cuvette with water. The temporal resolution of the apparatus is 10 ns, corresponding to the time necessary for the acoustic transients to travel through the probe beam focus. The rise time of the photodiode (Iskra MA 7590) and the storage oscilloscope (Tektronix 7834) is 2 and 1.2 ns, respectively.

An aperture with a diameter of 200 μm is placed directly in front of the photodiode. It transmits the probe beam but blocks out most of the light emitted from the plasma during optical breakdown. Thus the plasma spark is registered without overloading the photodiode and covering the probe signal. It serves as the zero mark for determining the time in which the acoustic transients propagate from the site of optical breakdown to the probe beam focus and to the microphones. The corresponding distances are obtained by multiplying the propagation times by the sound velocity in the liquid.

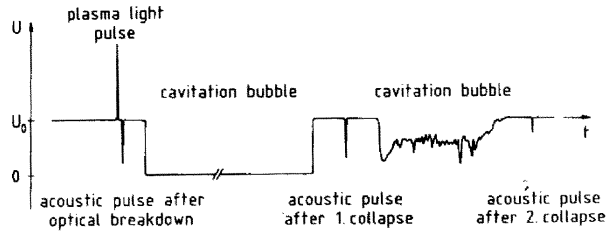

FIG. 4. Typical form of the photodiode signal caused by a laser-generated cavitation bubble.

The pressure amplitude of the acoustic transients is determined with hydrophone 1 (Celesco LC5-2) at a distance of about 20 mm from their emission center. The acoustic center of the transducer consists of a lead circonate ceramic cylinder with a length of 3.3 mm and a diameter of 2.5 mm. The sensitivity is 500 mV/bar and the rise time is 333 ns, corresponding to a frequency bandwidth of 1.5 MHz. The transducer signal is registered with a 10-MHz sampling rate by transient recorder 1 (Maurer ADAM TC 1008). This instrument has a storage capacity of 64 k(8 bit) which allows for tracking the sound emission throughout the whole lifetime of the cavitation bubbles. To dampen disturbing acoustic wave reflections, a sound absorber is attached to one side of the cuvette.

Figure 4 shows the typical form of the photodiode signal caused by a laser-generated cavitation bubble when the bubble radius is larger than the distance between the site of optical breakdown and the probe beam focus. In this case, the probe beam is temporarily blocked out by the bubble. The storage oscilloscope is externally pretriggered by a reference pulse from the ruby laser and then, after an adjustable delay time, triggered by the acoustic transient to be measured. This technique may fail when the photodiode signal differs from the typical form given in Fig. 4. Therefore, the correct triggering is checked by coupling the recording of the optical signal with the registration of the acoustical signal of a second pressure transducer. Hydrophone 2 (Imotec micropressure gauge) is based on piezoelectric polyvinylfluoride (PVDF) and has a sensitive area with a diameter of less than 0.5 mm.[39] The rise time is 145 ns and the sensitivity is about 2.5 mV/bar. The signal of the PVDF transducer placed at a distance of about 10 mm from the ruby laser focus is recorded with a 60-MHz sampling rate through transient recorder 2 (Sony/Tektronix 390 A/D).

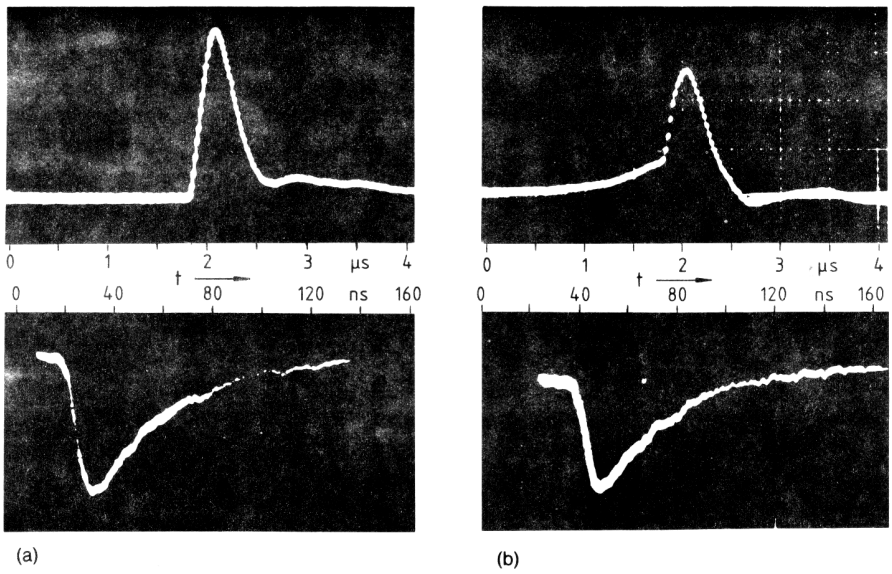

FIG. 5. Typical signals of the PVDF transducer (top) and of the photodetector (bottom) (a) after optical breakdown and (b) after cavitation bubble collapse. The distance between the emission center of the acoustic pulses and the probe was 1.2 mm for the optical and 8 mm for the acoustic measurement.

IV. RESULTS

A. Profile of the acoustic transients

Figure 5 shows typical signals of the PVDF transducer after the optical breakdown and after the spherical cavitation bubble collapse, together with the corresponding results of the optical detection. The pulse energy used to generate the bubbles was 200 mJ. The optical measurement reveals that the acoustic transients are much shorter than the rise time of the pressure transducer. For evaluating the optical measurements, first the distortion of the signal resulting from the nonlinearity of the $U(\phi)$ characteristic of the apparatus (see Fig. 2) is corrected. Then $p(t)/p_{max}$ is calculated by numerical integration. Some pressure profiles obtained in this way are given in Fig. 6.

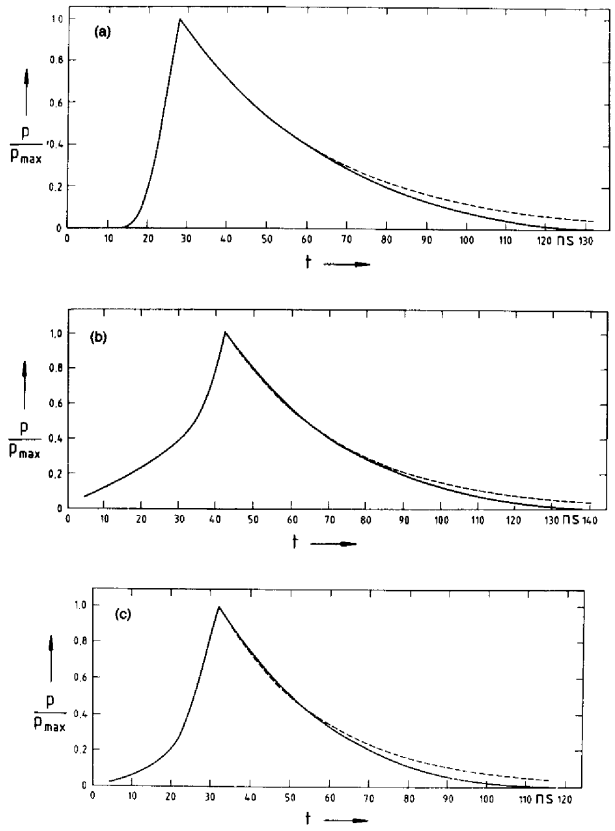

FIG. 6. Pressure profiles $p(t)/p_{max}$ of the acoustic transients (a) after optical breakdown and (b) and (c) after cavitation bubble collapse: —, experimentally determined profile; ---, exponential decrease. The measurement distance from the emission center of the acoustic pulses was 1.2 mm in (a) and (b) and 2.4 mm in (c). (a) and (b) correspond to the photodiode signals (a) and (b) in Fig. 5.

The duration τ (width at half-maximum) of the acoustic transients is about 25 ns both after breakdown and after bubble collapse. The same duration was observed for the acoustic pulses after the second bubble collapse. The pressure pulses after the optical breakdown feature a steep shock front, with a rise time of 10 ns. Since this value is equal to the temporal resolution of the apparatus, the actual shock front is probably even shorter. During cavitation bubble collapse, a relatively slow pressure rise occurs within 1–2 μs, followed by a shock front similar to that after breakdown. This result can be explained by the theoretical work of Hickling and Plesset[7] and Fujikawa and Akamatsu[13]: They found a strong pressure rise near the bubble wall during the last stages of the collapse and the evolution of a shock front during the rebound of the bubble. Behind the shock front, the pressure decreases nearly exponentially. This observation confirms the assumption about the pressure profile made in Sec. I.

Figure 7 shows an oscilloscope trace of a ruby laser pulse shape, together with the temporal behavior of the plasma luminescence during optical breakdown. The luminescence begins after the laser pulse intensity has reached the threshold for nonlinear absorption and plasma formation; remarkably, it already ceases when the laser pulse intensity still exceeds the threshold for breakdown. This is probably due to the rapid expansion of the plasma which reduces the electron density and the light absorption at the site of the ruby laser focus until the matter becomes transparent again and no more plasma is generated.[40] The average duration of the

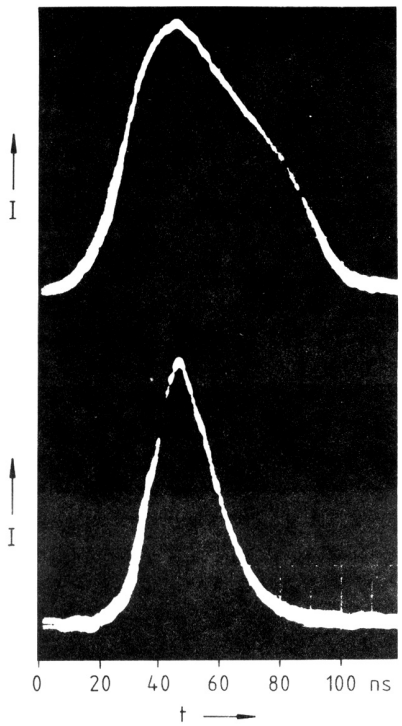

FIG. 7. Ruby laser pulse with 200-mJ pulse energy (top) and the light emitted by the laser induced plasma (bottom).

plasma luminescence after ruby laser pulses with 50 to 60 ns duration and 200-mJ pulse energy was 26 ns. The duration of the corresponding acoustic transients produced by the plasma expansion was nearly the same, namely, 24 ns (measured at a distance of 1.2 mm from the ruby laser focus). Thus the length of the pressure pulse seems to be correlated with the presence of the plasma rather than with the duration of the initiating laser light pulse.

In Fig. 8, the duration of the acoustic transients is plotted as a function of their distance from the emission center. Each value is the average of ten measurements, performed with a laser pulse energy of about 200 mJ. In the range investigated, reaching from a distance of 0.6–6 mm, the pulse duration was found to be nearly constant both for the transients after breakdown and after bubble collapse. A broadening of the pressure profile predicted by the propagation theory for finite amplitude waves[8,41] was not observed. This surprising result is probably due to the spherical form of the acoustic waves which leads to a rapid decrease of the pressure amplitude so that the domain of nonlinear sound propagation is limited to a small region around their emission center.

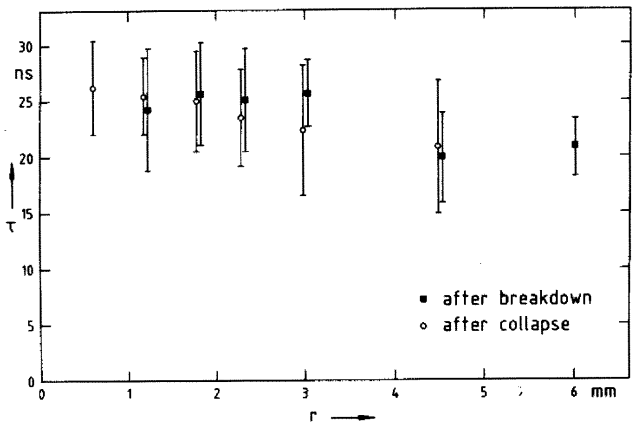

FIG. 8. Pulse duration τ of the acoustic transients after optical breakdown and after bubble collapse as a function of the distance r from their emission center.

The duration of the acoustic transients emitted during the bubble collapse near a solid boundary was the same as during spherical collapse when $\gamma \leqslant 0.75$ or $\gamma \geqslant 1.05$. In the range $0.75 < \gamma < 1.05$, the acoustic pulses were too weak to be detected with the optical technique. The signals from the pressure transducer, however, often have a duration of several microseconds, i.e., longer than the impulse response of the measuring instrument. It is not clear whether this is due to one long pressure pulse or to a series of short pulses which could not be resolved by the transducer. [The latter is suggested by the schlieren image in Fig. 21(b).]

B. Optical breakdown and spherical bubble collapse

Figure 9 shows the sound signal from a laser-produced cavitation bubble recorded with hydrophone 1. The collapse times T_{c_1}, T_{c_2}, and T_{c_3} for the first through third bubble collapse are proportional to the maximum bubble radius $R_{\max}$ before the respective collapse. The bubble radius can be deduced from the time distance $2T_c$ between the peaks of the pressure signal, making use of the relationship

$$R_{\max} = T_c/0.915[\rho/(p_{\text{stat}} - p_v)]^{1/2}, \tag{12}$$

derived by Rayleigh,[6] where ρ is the density of the liquid, p_{stat} is the static pressure, and p_v is the vapor pressure of the liquid. The energy E_B of the cavitation bubble is given by

$$E_B = \tfrac{4}{3}\pi(p_{\text{stat}} - p_v)R^3_{\max}. \tag{13}$$

The energy loss during bubble collapse is obtained by comparing the different values of the bubble energy before and after collapse. The peak pressure amplitude of the acoustic transients is calculated from the transducer signal and the pulse duration τ with the help of (8). In cases where τ could not be determined synchronously to the acoustic measure-

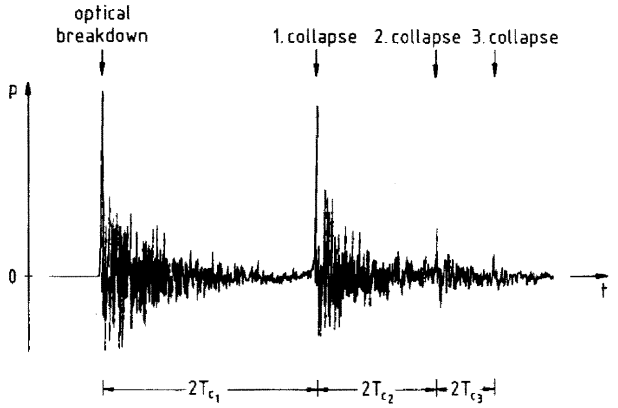

FIG. 9. Pressure-time signal of an oscillating laser-produced cavitation bubble; T_c is the collapse time of the bubble.

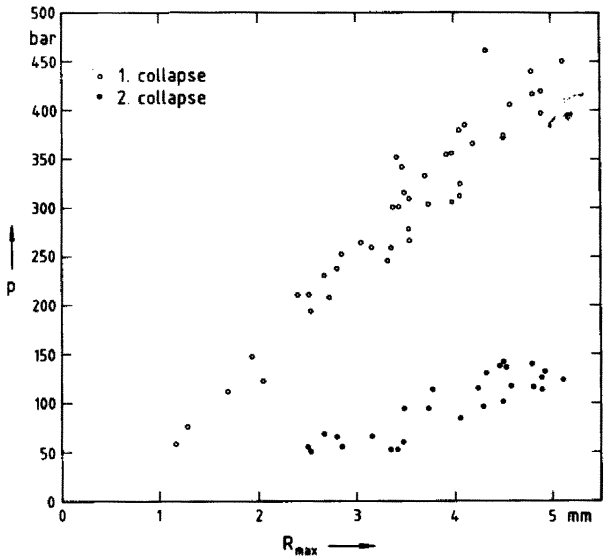

FIG. 10. Peak pressure p of the acoustic transients emitted during the first and second bubble collapse as a function of the maximum bubble radius R_{max}. The pressure values are normalized to a distance $r = 10$ mm from the bubble center.

ment, we calculated the peak pressure assuming a pulse duration of $\tau = 20$ ns at the site of the transducer. This value results from extrapolating the data given in Fig. 8 to a distance of 20 mm. The energy of a spherical acoustic transient as derived by Cole[41] is

$$E_s = \frac{4\pi r^2}{\rho c} \int p^2 \, dt, \tag{14}$$

where c denotes the sound velocity in the liquid and r is the distance between the pressure transducer and the emission center of the transient. The sum of the cavitation bubble energy and the energy of the pressure pulse after optical breakdown is a measure for the fraction of laser light energy that is converted into mechanical energy.

In Fig. 10, the peak pressure of the acoustic transients emitted during the first and second cavitation bubble collapse is plotted versus the maximum bubble radius. The pressure values refer to a distance r of 10 mm between the bubble center and the site of measurement. The acoustic signals used for evaluation have been selected to exclude as far as possible bubbles with deviations from the spherical form. Those bubbles are indicated by multiple pressure pulses emitted during optical breakdown and collapse easily visible with the optical detection technique. In the domain of linear sound propagation when the pulse broadening and dissipation can be neglected, the amplitude of a spherical acoustic wave is inversely proportional to the distance r. Hickling and Plesset,[7] as well as Fujikawa and Akamatsu,[13] have shown by numerical calculations that the $1/r$ law is also approximately true for the nonlinear domain in the direct vicinity of the collapse center. In this region, the effects due to the dissipation of sound energy are compensated by the development of the shock front. Timm[42] has found by means of high-speed photography with one million frames/s that the minimum radius of laser-produced cavitation bubbles during spherical collapse is about 50 μm. Taking the experimentally observed

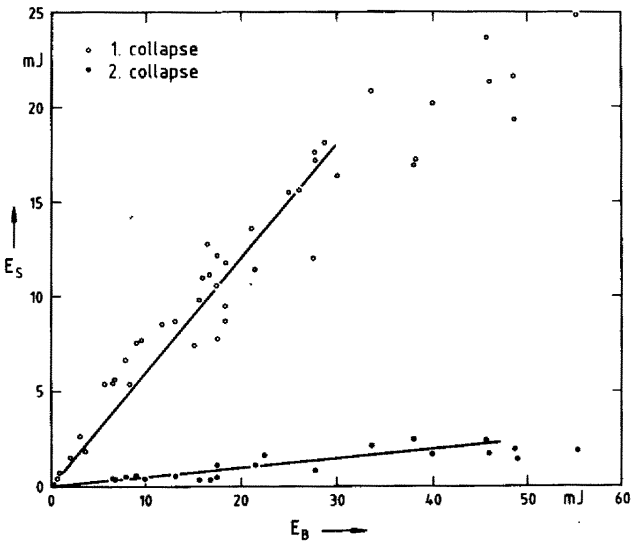

FIG. 11. Energy E_s of the acoustic transients produced during the first and second bubble collapse plotted versus the bubble energy E_B.

pressure amplitudes as a basis and using the $1/r$ law, the pressure at $r = 50\,\mu$m is calculated to be 60 kbar when $R_{max} = 3.5$ mm. Thus the maximum pressure developed inside the bubble during collapse is about 60 kbar.

Figure 11 shows that the energy of the acoustic transients increases proportionally to the energy of the cavitation bubbles as long as the bubble energy does not exceed 30 mJ, corresponding to a radius of 4 mm. Larger bubbles can only be produced with a high laser pulse energy of more than 300 mJ: Therefore, they probably frequently feature deviations from the spherical form because of multiple optical breakdowns in the region surrounding the ruby laser focus. Since these deviations grow during bubble collapse,[43,44] the bubble implodes less violently than during spherical collapse, and the sound emission is diminished.

The average energy loss of the cavitation bubble during their first collapse is 84%. It appears from Fig. 12 that the

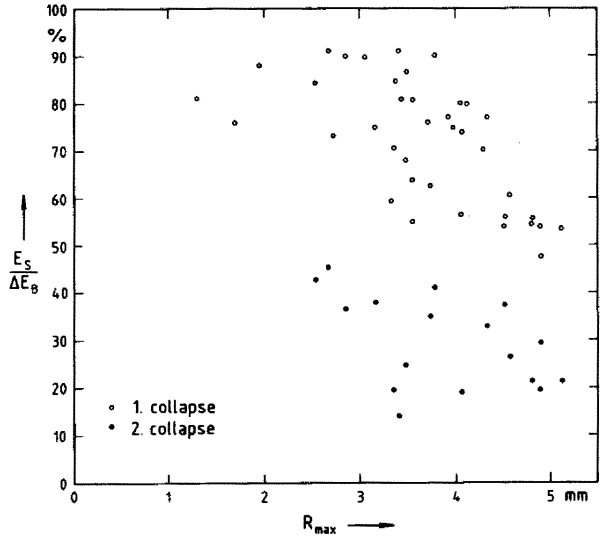

FIG. 12. Fraction of the energy loss ΔE_B during the bubble collapse which is converted into acoustic energy E_s, plotted versus the maximum bubble radius R_{max}.

major part of it—maximal 90% and 73% on an average—is due to the emission of sound. Heat conduction and viscosity seem to play only a minor part in damping the oscillations of transient spherical bubbles. These findings are in good agreement with the theoretical work reported in Refs. 11–13 as well as with the experimental work of Teslenko.[14] The results of Hentschel and Lauterborn,[15] who claimed that only about 1.2% of the bubble energy is converted into acoustic energy, were obtained without properly taking into account the limited bandwidth of the pressure transducer. The importance of sound emission decreases for large bubbles with $R_{max} > 4$ mm because of the above-mentioned deviations from spherical shape. Since almost all bubbles lose their spherical shape during rebound, the sound emission is generally less important in the second collapse than in the first collapse.

The pressure pulses emitted during optical breakdown generally have approximately the same amplitude as those produced during the collapse of the subsequently emerging cavitation bubble. Thus the acoustic transients observed after bubble generation and collapse have similar amplitude, duration, and profile (see Figs. 6 and 8), although the physical processes leading to their emission are quite different. However, both optical breakdown and bubble collapse lead to an extremely high temperature and pressure within a very small volume of not more than 100-μm diam. Therefore, it is quite reasonable that the subsequent expansion of the compressed matter causes similar effects. Whereas the energy for the acoustic transient after breakdown is delivered from the laser pulse, it is supplied by the energy stored in the bubble for the pressure pulse after collapse. This leads to a reduction of the bubble energy after rebound and, consequently, of the energy available for sound emission during second collapse.

No pronounced relationship has been observed between the energy of the ruby laser pulses and the acoustic energy after breakdown or the energy of the cavitation bubble. The conversion efficiency for light energy into mechanical energy fluctuated between 2% and 40%, with an average of 17%. One reason for the fluctuations is that the breakdown threshold depends on the presence of small impurities in the focal region of the laser beam, which may differ from pulse to pulse. Another reason may be given by the complex spatial mode structure of the ruby laser which also varies from pulse to pulse, resulting in "hot spots" in different extent and at different locations. A much more regular behavior was observed in experiments with the TEM_{00} Nd:YAG laser. This can be seen in Fig. 13, where each value is the average of ten measurements. The energy of the acoustic transients generated upon optical breakdown is proportional to the laser pulse energy after the breakdown threshold of 0.7 mJ is exceeded. Similar results have been reported by Schmidt-Kloiber and Reichel.[46] Figure 14 shows that, for Nd:YAG laser pulses with more than 4 mJ, about 3.5% of the light energy is converted into the energy of the first acoustic wave and about 7.5% is converted into the energy of the bubble oscillation. For smaller values of the laser pulse energy, the conversion efficiency decreases until it drops to zero at the breakdown threshold. These findings are contradictory to the results of Teslenko,[45] who reported that up to 30% of the initial energy

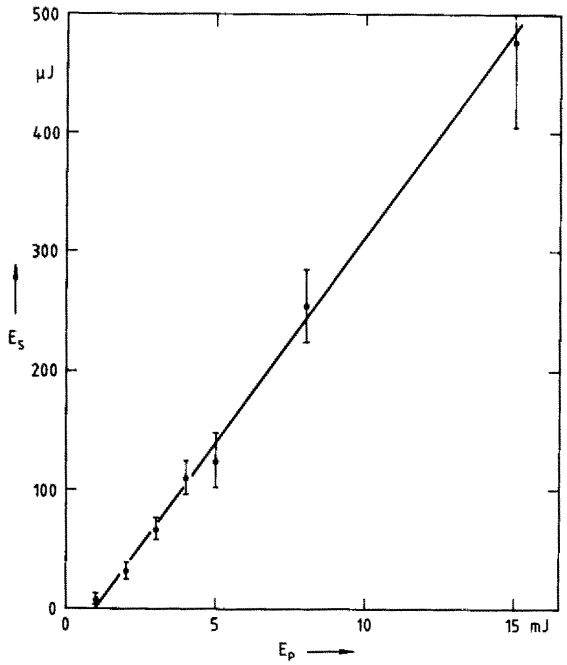

FIG. 13. Energy E_s of the acoustic transients produced during optical breakdown as a function of the laser pulse energy E_p. The measurements were performed with the TEM_{00} Nd:YAG laser.

of the light pulse is transported by the first acoustic wave, with 10% going for the bubble pulsations. Since the acoustic transients after breakdown and after bubble collapse have similar pressure amplitudes and duration, the bubble energy represents an upper limit for the energy values of both transients. Teslenko's results are therefore questionable—probably due to an overestimation of the pulse duration used for the calculation of the energy of the acoustic transients.

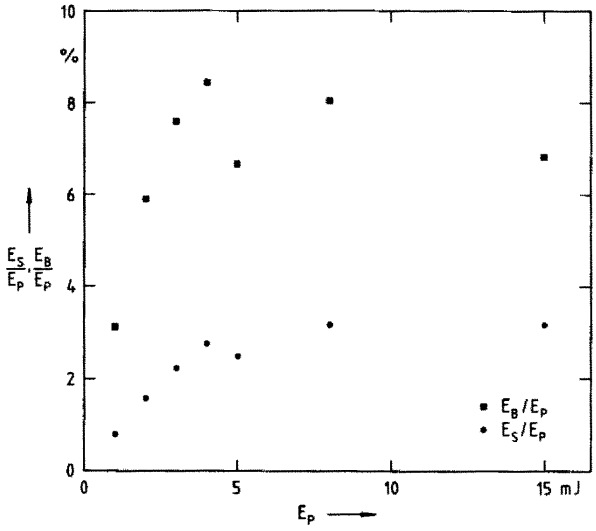

FIG. 14. Fraction of the laser pulse energy converted into the energy of the acoustic transient after breakdown (E_s/E_p) and into the energy of the cavitation bubble (E_B/E_p), both plotted versus the laser pulse energy. The measurements were performed with the TEM_{00} Nd:YAG laser.

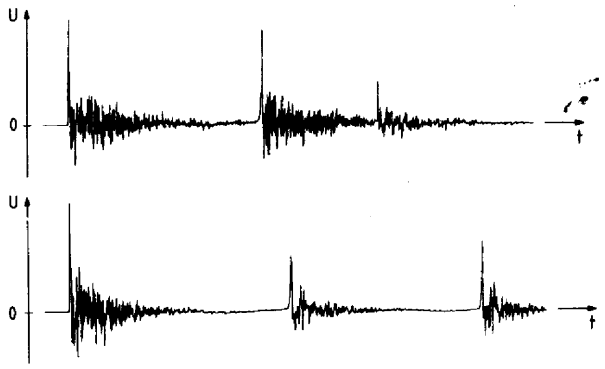

FIG. 15. Sound signal from laser-produced cavitation bubbles when the collapse is spherical (top) and when it occurs near a solid boundary with $\gamma = 1.4$ (bottom). In both cases, the maximum bubble radius is 4.4 mm.

C. Bubble collapse near a solid boundary

In Fig. 15, the sound signal from a spherically collapsing cavitation bubble is compared with the signal from a bubble that collapses near a solid boundary. The solid boundary leads to a decrease of the pressure amplitude after the first bubble collapse and to an increase of the pressure produced during the second collapse. Moreover, the boundary causes a prolongation of the collapse time so that (12) does not hold any longer. The maximum bubble radius may still be determined from the collapse time, if the prolongation factor against Rayleigh's collapse time for the spherical collapse is known. The knowledge of the maximum bubble radius before the first collapse and after rebound makes it possible to calculate the bubble energy and the energy loss during collapse. The dependence of the prolongation factor k on the dimensionless distance γ between bubble and boundary was experimentally investigated by evaluating a large number of high-speed photographical series of the bubble dynamics.[47] The result is shown in Fig. 16, together with a theoretical curve derived from a perturbation analysis by Rattray (see Ref. 48).

Figure 17 shows the pressure amplitude of the acoustic transient after the first bubble collapse as a function of γ. The pressure was normalized to a distance of 10 mm from the collapse center. Since the sound emission during aspherical bubble collapse may be anisotropic, two series of measurements were performed with the pressure transducer placed above the bubble and the boundary in one series and beside the bubble in the other series. The average bubble radius was $R_{max} = 3.5 \pm 0.6$ mm in both cases. Thus the pressure val-

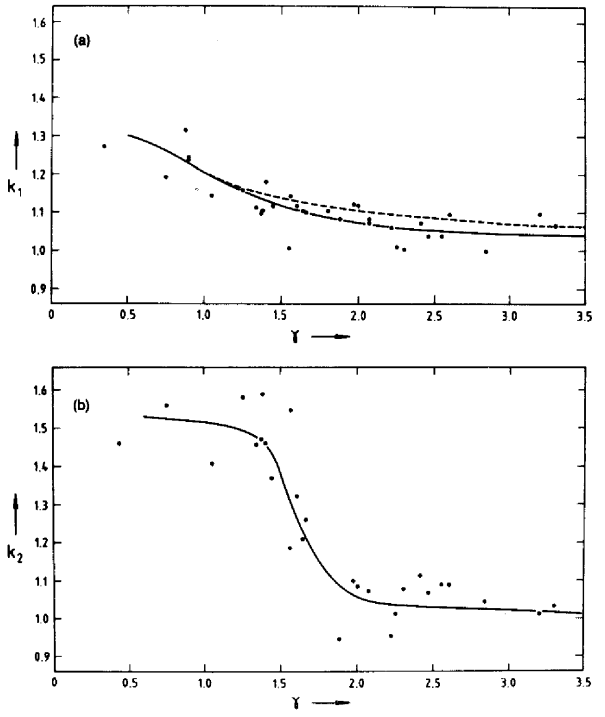

FIG. 16. Prolongation factors k_1 and k_2 versus the time for spherical bubble collapse as a function of γ (a) for the first collapse and (b) for the second collapse: ---, theoretical curve derived by Rattray (see Ref. 48); —, curve fitted to the values obtained experimentally.

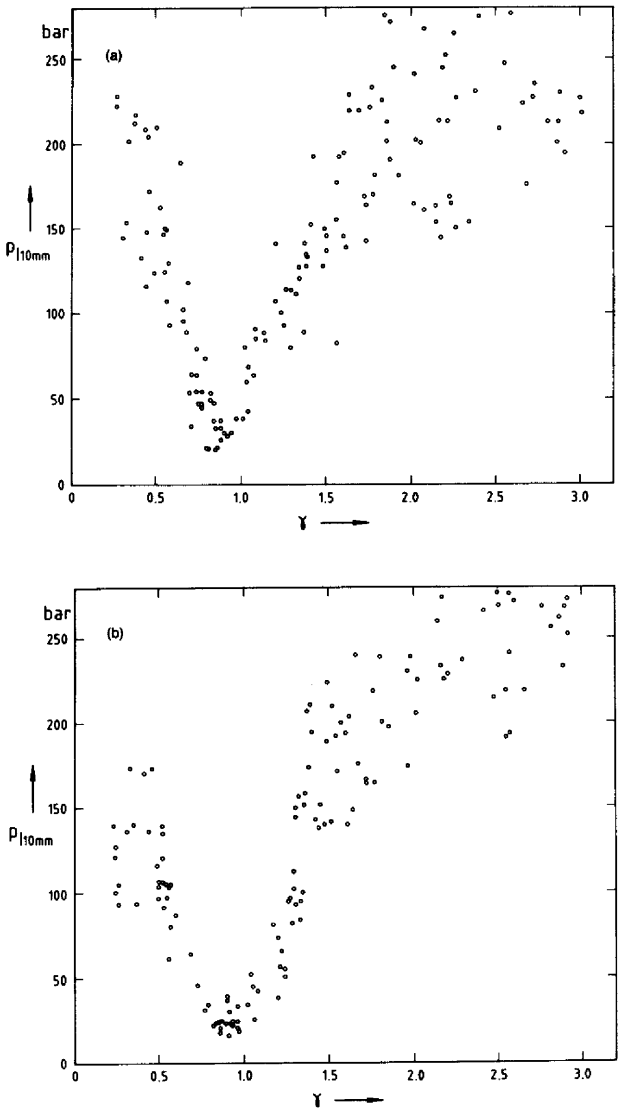

FIG. 17. Pressure amplitude p after the first bubble collapse as a function of γ. The pressure values refer to a distance of 10 mm from the collapse center; $R_{max} = 3.5 \pm 0.6$ mm. The hydrophone was placed (a) above and (b) beside the bubble.

ues for a certain γ value may belong to bubbles of slightly different size that produce acoustic transients of slightly different amplitudes. This partly masks the law governing the relationship between sound emission and the normalized distance γ. It has been shown for the spherical bubble collapse with $R_{max} < 4$ mm that the energy of the acoustic pulses is proportional to the bubble energy (see Fig. 11). Assuming this proportionality to be true also for each γ value upon aspherical collapse, the dependence of the sound emission from γ is elucidated by normalizing the energy of the acoustic pulse with the bubble energy, as shown in Fig. 18. Figure 19 shows the energy loss of the cavitation bubble during the first collapse. The importance of sound emission in damping the bubble oscillations for aspherical collapse can be estimated by relating the energy of the acoustic transient produced during the collapse to the energy loss of the bubble (see Fig. 20). The curves have been fitted to the measurement values in order to facilitate the comparison of both measurement series with different microphone positions.

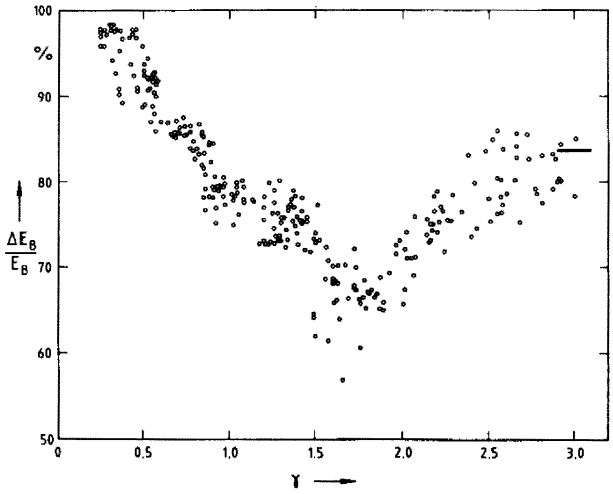

FIG. 19. Relative energy loss $\Delta E_B / E_B$ during the first bubble collapse as a function of γ. The horizontal bar marks the value for the spherical collapse.

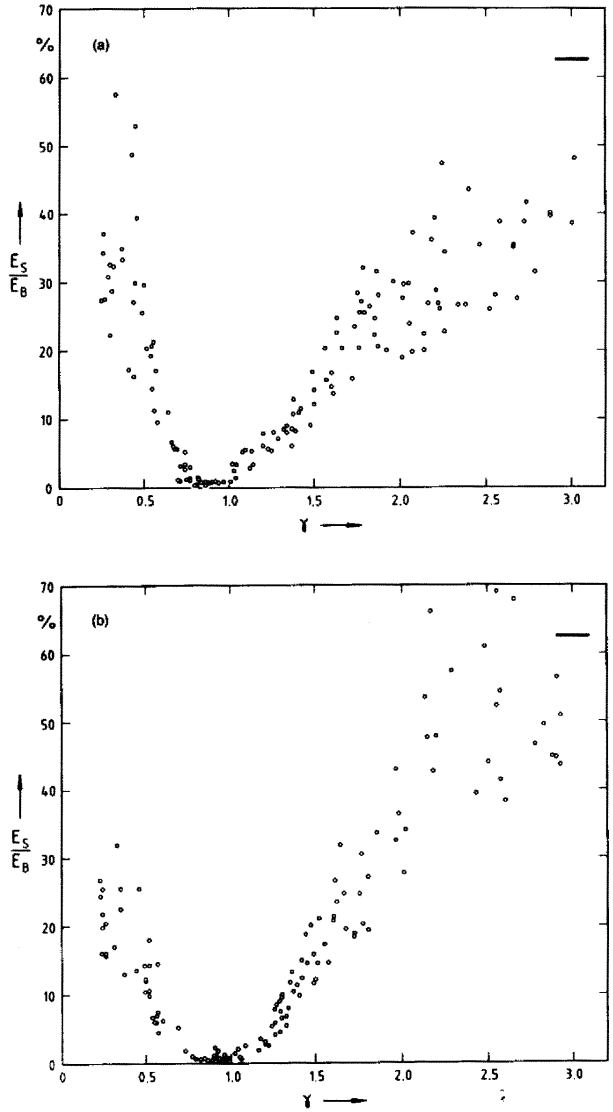

FIG. 18. Energy E_s of the acoustic transient after the first bubble collapse normalized with the bubble energy E_B, plotted versus γ. Hydrophone placed (a) above and (b) beside the bubble. The horizontal bar marks the average value upon spherical collapse.

Looking at Figs. 17–20, the strong drop of sound emission for γ values of about $\gamma = 0.9$ attracts attention. This behavior was also observed by Naudé and Ellis[17] and Tomita and Shima[19]; it is due to the modification of the bubble collapse by the jet formation. For large γ values, the collapse is almost spherical and the liquid jet does not emerge before the rebound of the bubble (see Ref. 21). Therefore, the liquid moves almost radially toward the collapse center, leading to a violent collapse with strong sound emission. In the range around $\gamma = 0.9$, the jet appears before the bubble has

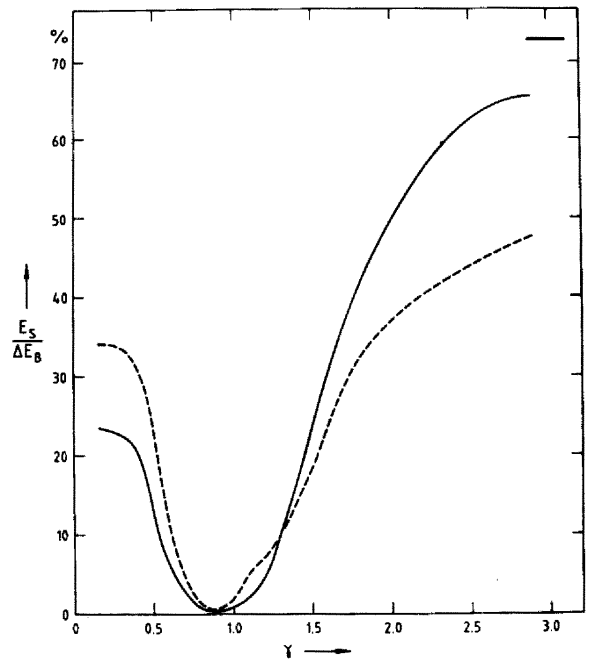

FIG. 20. Fraction of the energy loss ΔE_B during the first bubble collapse which is converted into acoustic energy E_s, plotted versus γ. The average value for the spherical collapse is marked by the horizontal bar: —, hydrophone placed above the bubble; ---, hydrophone placed beside the bubble.

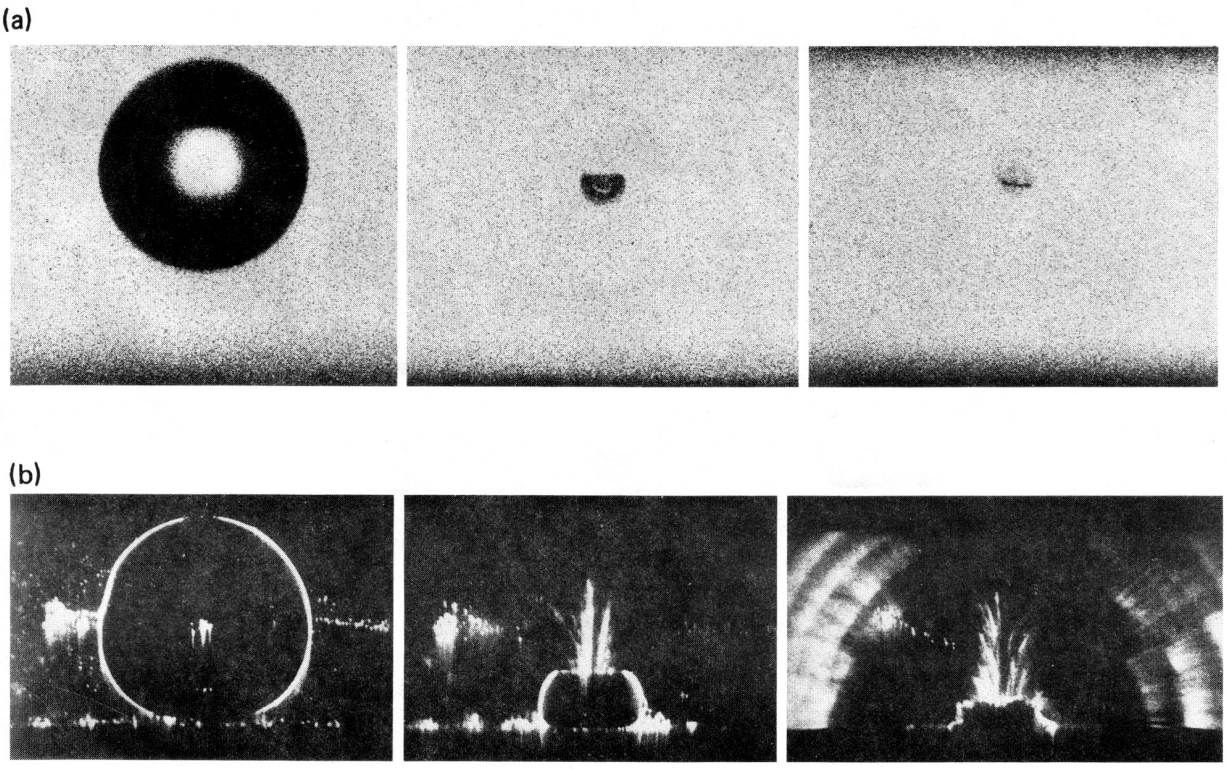

FIG. 21. Bubble collapse at different distances between bubble and boundary: (a) $\gamma = 2.2$ and $R_{max} = 2.7$ mm; (b) $\gamma = 0.96$ and $R_{max} = 3.9$ mm. The bubble is shown at maximum expansion and at the first collapse in the left and right frames, respectively. The middle frame was taken 1 μs before collapse in (a) and 30 μs before collapse in (b). The solid boundary is located at the bottom of each frame.

achieved its minimum extension. The jet penetrates the bubble wall at the side of the solid boundary and, during the last stages of the collapse, a vortex ring with a hollow toroidal core is formed which moves toward the boundary.[47] The kinetic energy of the radial flow into the bubble is thereby partly transformed into energy of rotation. Hence, the bubble content becomes less compressed than in the case of large γ values, and the sound emission is diminished.[49]. The dependence of minimum bubble size from γ is illustrated by the pictures in Fig. 21 which were taken from a high-speed photographical series with 20 000 frames/s. The pictures were photographed with diffuse illumination from the back in Fig. 21(a) and with a schlieren technique in 21(b).[47] For $\gamma \to 0$, the sound emission increases again, although the jet is still formed very early during the collapse, similar to the case of $\gamma = 0.9$. However, if γ is very small, the bubble is nearly hemispherical and its center can hardly move during collapse. Therefore, no pronounced vortex ring is developed in spite of the outward flow on the surface of the solid boundary following jet impact. The flow is directed toward the bubble center for most parts of the bubble surface, as in the spherical collapse. This causes a strong compression of the bubble content and the generation of an intense pressure pulse. Figure 20 shows that for $\gamma \leqslant 2.0$ the damping of the bubble oscillation is predominantly caused by mechanisms other than the emission of sound—probably mainly by viscous damping due to the turbulent jet flow and the ring vortex. For $0.6 \leqslant \gamma \leqslant 1.3$, the acoustic energy accounts for less than 10% of the energy loss in the first bubble collapse.

It is evident from Fig. 20 that the sound emission near a solid boundary is anisotropic. For $\gamma \leqslant 1.3$, the pressure amplitudes are much higher in the direction perpendicular to the boundary than beside the bubble. This is probably due to the funnel-shaped jet acting as a sound projector. It is reasonable that the mechanism becomes less effective with growing γ when the jet only appears during bubble rebound. We cannot explain, however, why for $\gamma \geqslant 1.3$ the sound radiation is stronger in the horizontal than the vertical direction.

Figure 19 demonstrates that for $0.85 \leqslant \gamma \leqslant 2.5$ the energy loss during the first collapse is smaller than upon spherical collapse. This coincides with a remarkable increase of sound emission during the second collapse (see Fig. 22) which for $0.75 \leqslant \gamma \leqslant 1.4$ is stronger than the sound radiation after the first collapse. After rebound, the bubbles have a toroidal form, with the torus usually disintegrating into several parts that collapse separately, emitting various acoustic transients.[47] The irregularity of this process leads to the strong scatter of the measurement values in Fig. 22.

The highest pressure amplitudes at the solid boundary are achieved when γ is very small. One can read from Fig. 17 that, for $\gamma = 0.2$ and $R_{max} = 3.5$ mm, the pressure amplitude after the first bubble collapse is about 150 bar at a distance of 10 mm from the collapse center. This value is the average of the data belonging to both hydrophone positions. We found by high-speed photography that the minimum size of the collapsed bubble corresponds to a bubble with a radius of about 0.6 mm.[47] Calculation of the pressure value at this radius, proceeding from the measured amplitude, yields the

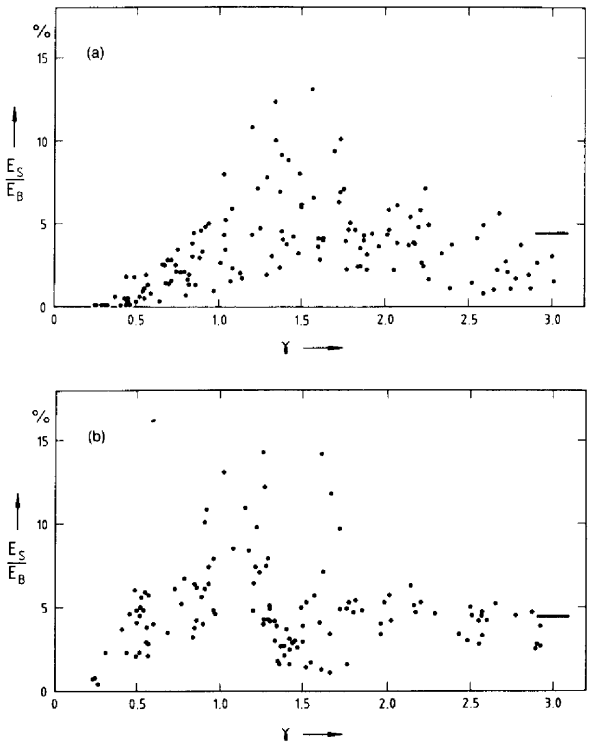

FIG. 22. Energy E_s of the acoustic pulse after the second bubble collapse, related to the bubble energy E_B, plotted versus γ. Hydrophone placed (a) above the bubble and (b) beside the bubble. The horizontal bar marks the value for spherical collapse.

value of 2.5 kbar for the maximum pressure inside the bubble and at the boundary. This result agrees well with the findings of Jones and Edwards (10 kbar for $\gamma = 0$ and $R_{max} = 4.9$ mm),[50] but it is almost 17 times higher than the value reported by Tomita and Shima (150 bar for $\gamma = 0.2$ and $R_{max} = 3.5$ mm).[19] The deviation can be explained by the fact that Tomita and Shima employed a pressure transducer with a rise time of 1 μs without considering the much shorter duration of the pressure pulses to be measured.

V. CONCLUSION

The acoustic transient generation by laser-produced cavitation bubbles has been investigated with optical and acoustic methods. The optical measurements revealed that the pressure profile of the acoustic transients has the form of an exponential impulse with a rise time of less than 10 ns. The duration of the pressure pulses (their width at half-maximum) has been found to be 20–30 ns in the range of 0.6–6 mm from the emission center of the pulses. The pressure amplitudes are approximately the same for the acoustic pulses generated during optical breakdown and bubble collapse. During breakdown, about 3.5% of the laser light energy is converted into acoustic energy and about 7.5% is converted into the energy of the cavitation bubble. During spherical bubble collapse, a maximum pressure of about 60 kbar is developed inside a bubble with $R_{max} = 3.5$ mm, and an average of 73% of the bubble energy is transformed into acoustic energy. Thus we could confirm that the sound emission is the most important damping mechanism in the collapse of transient spherical cavitation bubbles in water, as has been pointed out by previous theoretical papers.[11–13]

The sound emission during the bubble collapse near a solid boundary is strongly dependent on the dimensionless distance γ between the bubble and the boundary: For $0.6 \leqslant \gamma \leqslant 1.3$, it contributes with less than 10% to the damping of the bubble oscillations and for $0.8 \leqslant \gamma \leqslant 0.95$ it contributes with even less than 1%. The highest pressure amplitudes at the solid boundary are achieved for $\gamma \to 0$. For $\gamma = 0.2$ and $R_{max} = 3.5$ mm, the maximum pressure inside the bubble is about 2.5 kbar. Therefore, cavitation erosion is mainly caused by bubbles attached to the boundary. Moreover, in this case there is no water film between bubble and boundary cushioning the impact of the high-speed liquid jet.

Lush *et al.*[51] have found that the dynamic hardness of aluminium which they assume to be representative of the plastic flow stress is 13.7 kbar. Since an aluminium surface exposed to cavitation will be eroded, the pressure values at the surface must locally be higher than the value of 2.5 kbar inside the collapsed bubbles. A possible mechanism for producing higher pressures is the impact of the liquid jet, but Lush *et al.* calculated a jet speed of 550 m/s necessary to generate a water hammer pressure strong enough to deform aluminium. Jets with such a high velocity have not yet been observed during the collapse of single cavitation bubbles in a liquid without a flow; however, they can possibly be formed if the bubble collapse occurs in a flow directed toward the boundary[52] or when it is accelerated by acoustic transients emitted from adjacent bubbles, which frequently happens in collapsing cavitation bubble clouds.[53–55] The investigation of the interaction of gas bubbles with acoustic transients[19,56,57] has shown that the acoustic transients can induce very fast jets. It is likely that the jets are even faster when the acoustic pulses interact with already collapsing cavitation bubbles. The exploration of this mechanism seems to be a promising task for the explanation of unwanted cavitation erosion, as well as for the enhancement of the intended erosion effects in laser lithotripsy.

[1] G. A. Askar'yan, A. M. Prokhorov, G. F. Chanturiya, and G. P. Shipulo, "The effects of a laser beam in a liquid," Sov. Phys. JETP **17**, 1463–1465 (1963).

[2] R. G. Brewer and K. E. Rieckhoff, "Stimulated Brillouin scattering in liquids," Phys. Rev. Lett. **13**, 334–336 (1964).

[3] E. F. Carome, C. E. Moeller, and N. A. Clark, "Intense ruby-laser-induced acoustic impulse in liquids," J. Acoust. Soc. Am. **40**, 1462–1466 (1966).

[4] C. E. Bell and J. A. Landt, "Laser-induced high-pressure shock waves in water," Appl. Phys. Lett. **10**, 46–48 (1967).

[5] P. A. Barnes and K. E. Rieckhoff, "Laser-induced underwater sparks," Appl. Phys. Lett. **13**, 282–284 (1968).

[6] J. W. Rayleigh, "On the pressure developed in a liquid during the collapse of a spherical cavity," Philos. Mag. **34**, 94–98 (1917).

[7] R. Hickling and M. S. Plesset, "Collapse and rebound of a spherical bubble in water," Phys. Fluids **7**, 7–14 (1964).

[8] I. B. Esipov and K. A. Naugol'nykh, "Expansion of a spherical cavity in a liquid," Sov. Phys. Acoust. **18**, 194–197 (1972).

[9] U. Radek, "Kavitationserzeugte Druckimpulse und Materialzerstörung," Acustica **26**, 270–283 (1972).

[10]K. Hinsch and E. Brinkmeyer, "Investigation of very short cavitation shock waves by coherent optical methods," SPIE **97**, 166–171 (1976).
[11]K. J. Ebeling, "Zum Verhalten kugelförmiger, lasererzeugter Kavitationsblasen in Wasser," Acustica **40**, 229–239 (1978).
[12]T. Nishiyama and M. Akaizawa, "Pressure waves produced by the collapse of a spherical bubble," Technol. Rep. Tohoku Univ. **44**, 579–602 (1979).
[13]S. Fujikawa and T. Akamatsu, "Effects of the non-equilibrium condensation of vapour on the pressure wave produced by the collapse of a bubble in a liquid," J. Fluid Mech. **97**, 481–512 (1980).
[14]V. S. Teslenko, "Experimental investigation of bubble collapse at laser-induced breakdown in liquids," in *Cavitation and Inhomogeneities in Underwater Acoustics*, edited by W. Lauterborn (Springer, Berlin, 1980).
[15]W. Hentschel and W. Lauterborn, "Acoustic emission of single laser-produced cavitation bubbles and their dynamics," Appl. Sci. Res. **38**, 225–230 (1982).
[16]T. B. Benjamin and A. T. Ellis, "The collapse of cavitation bubbles and the pressures thereby produced against solid boundaries," Philos. Trans. R. Soc. London Ser. A **260**, 221–240 (1966).
[17]C. F. Naudé and A. T. Ellis, "On the mechanism of cavitation damage by nonhemispherical cavities collapsing in contact with a solid boundary," Trans. ASME Ser. D, J. Basic Eng. **83**, 648–656 (1961).
[18]A. Shima, K. Takayama, and Y. Tomita, "Mechanism of impact pressure generation from spark-generated bubble collapse near a wall," AIAA J. **21**, 55–59 (1983).
[19]Y. Tomita and A. Shima, "Mechanisms of impulsive pressure generation and damage pit formation by bubble collapse," J. Fluid Mech. **169**, 535–564 (1986).
[20]W. Lauterborn, "Kavitation durch Laserlicht," Acustica **31**, 51–78 (1974).
[21]W. Lauterborn and H. Bolle, "Experimental investigation of cavitation-bubble collapse in the neighbourhood of a solid boundary," J. Fluid Mech. **72**, 391–399 (1975).
[22]F. Fankhauser, P. Roussel, and J. Steffen, "Clinical studies on the efficiency of high power laser radiation upon some structures of the anterior segment of the eye," Int. Ophthalmol. **3**, 129–139 (1981).
[23]D. Aron-Rosa, *Pulsed YAG Laser Surgery* (Slack, Thorofare, NJ, 1983).
[24]R. F. Steinert and C. A. Puliafito, *The Nd-YAG Laser in Ophthalmology. Principles and Clinical Applications of Photodisruption* (Saunders, Philadelphia, 1985).
[25]H. Schmidt-Kloiber, E. Reichel, and H. Schöffmann, "Laserinduced shock-wave lithotripsy," Biomed. Technik **30**, 173–181 (1985).
[26]F. Frank, A. Hoffstetter, E. Keiditsch, and F. Wondrazek, "Experimental investigation of neodymium YAG laser induced shock waves for lithotripsy," Eur. Urol. **12**, 54–57 (1986).
[27]P. Teng, N. S. Nishioka, R. R. Anderson, and T. F. Deutsch, "Optical studies of pulsed-laser fragmentation of biliary calculi," Appl. Phys. B **42**, 73–78 (1987).
[28]A. Vogel, W. Hentschel, J. Holzfuss, and W. Lauterborn, "Cavitation bubble dynamics and acoustic transient generation in ocular surgery with pulsed neodymium: YAG lasers," Ophthalmology **93**, 1259–1269 (1986).
[29]E. Reichel, H. Schmidt-Kloiber, H. Schöffmann, G. Dohr, and A. Eherer, "Interaction of short laser pulses with biological structures," Opt. Laser Technol. **19**, 40–44 (1987).
[30]J. G. Fujimoto, W. Z. Lin, E. P. Ippen, C. A. Puliafito, and R. F. Steinert, "Time-resolved studies of Nd:YAG laser-induced breakdown," Invest. Ophthalmol. Vis. Sci. **26**, 1771–1777 (1985).
[31]H. Stepp, E. Hofbauer, M. Seeberger, and E. Unsöld, "Fast pressure measurements on shock waves intraocularly generated by picosecond Nd:YAG-laser pulses," Laser Medizin Chirurgie **1**, 151–154 (1985).
[32]F. V. Bunkin and V. M. Komissarov, "Optical excitation of sound waves," Sov. Phys. Acoust. **19**, 203–211 (1973).
[33]W. Eisenmenger, "Experimentelle Bestimmung der Stossfrontdicke aus dem akustischen Frequenzspektrum elektromagnetisch erzeugter Stosswellen in Flüssigkeiten bei einem Stossdruckbereich von 10 atm bis 100 atm," Acustica **14**, 188–204 (1964).
[34]R. Bracewell, *The Fourier Transform and Its Applications* (McGraw-Hill, New York, 1965).
[35]G. P. Davidson and D. C. Emmony, "A schlieren probe method for the measurement of the refractive index profile of a shock wave in a fluid," J. Phys. E: Sci. Instrum. **13**, 92–97 (1980),
[36]B. Sullivan and A. C. Tam, "Profile of laser-produced acoustic pulse in a liquid," J. Acoust. Soc. Am. **75**, 437–441 (1984).
[37]M. W. Sigrist, "Laser generation of acoustic waves in liquids and gases," J. Appl. Phys. **60**, R83–R121 (1986).
[38]K. Vedam and P. Limsuwan, "Piezo-optic behaviour of water and carbon tetrachloride under high pressure," Phys. Rev. Lett. **35**, 1014–1016 (1975).
[39]M. Müller and M. Platte, "Einsatz einer breitbandigen Piezodrucksonde auf PVDF-Basis zur Untersuchung konvergierender Stosswellen in Wasser," Acustica **58**, 215–222 (1985).
[40]J. F. Ready, *Effects of High-power Laser Radiation* (Academic, New York, 1971).
[41]R. H. Cole, *Underwater Explosions* (Princeton U.P., Princeton, 1948).
[42]W. Lauterborn and R. Timm, "Bubble collapse at a million frames per second," in *Cavitation and Inhomogeneities in Underwater Acoustics*, edited by W. Lauterborn (Springer, Berlin, 1980).
[43]H. W. Strube, "Numerische untersuchungen zur stabilität nichtsphärisch schwingender blasen," Acustica **25**, 289–303 (1971).
[44]M. S. Plesset, "Bubble dynamics and cavitation erosion," in *Proceedings of the Symposium on Finite-Amplitude Wave Effects in Fluids*, edited by L. Bjørnø (IPC Science and Technology, Guildford, 1974), pp. 203–209.
[45]V. S. Teslenko, "Investigation of photoacoustic and photohydrodynamic parameters of laser breakdown in liquids," Sov. J. Quantum Electron. **7**, 981–984 (1977).
[46]H. Schmidt-Kloiber and E. Reichel, "Die Abhängigkeit der Druckamplitude einer Stosswelle von der Feldstärke beim laserinduzierten Durchbruch in Flüssigkeiten," Acustica **54**, 284–288 (1984).
[47]A. Vogel, "Optische und akustische Untersuchungen der Dynamik lasererzeugter Kavitationsblasen nahe fester Grenzflächen," Ph.D. thesis (Univ. of Göttingen, Göttingen, 1987).
[48]M. S. Plesset and R. B. Chapman, "Collapse of an initially spherical vapour cavity in the neighbourhood of a solid boundary," J. Fluid Mech. **47**, 283–290 (1971).
[49]G. L. Chahine and Ph. G. Genoux, "Collapse of a caviting vortex ring," Trans. ASME J. Fluids Eng. **105**, 400–405 (1983).
[50]I. R. Jones and D. H. Edwards, "An experimental study on the forces generated by the collapse of transient cavities in water," J. Fluid Mech. **7**, 596–609 (1960).
[51]P. A. Lush, R. J. K. Wood, and L. J. Carpanini, "Pitting in soft aluminium produced by spark-induced cavitation bubbles," in *Proceedings of the 6th International Conference on Erosion by Liquid and Solid Impact*, edited by J. E. Field and N. S. Corney (Cavendish Laboratory, Cambridge, 1983), Paper No. 5.
[52]A. T. Ellis and J. E. Starret, "A study of cavitation bubble dynamics and resultant pressures on adjacent solid boundaries," *Proceedings of the 2nd International Conference on Cavitation* (IMECHE, London, 1983), Paper No. C190/83.
[53]B. Vyas and C. M. Preece, "Stress produced in a solid by cavitation," J. Appl. Phys. **47**, 5133–5138 (1976).
[54]K. A. Mørch, "On the collapse of cavity clusters in flow cavitation," in *Cavitation and Inhomogeneities in Underwater Acoustics*, edited by W. Lauterborn (Springer, Berlin, 1980).
[55]G. L. Chahine, "Pressure generated by a bubble cloud collapse," Chem. Eng. Comm. **28**, 355–367 (1984).
[56]W. Lauterborn, "High speed photography of laser-induced breakdown in liquids," Appl. Phys. Lett. **21**, 27–29 (1972).
[57]N. Sanada, J. Ikeuchi, and K. Takayama, "Interaction of an air bubble with a shock wave generated by a micro-explosion in water," *Proceedings of the International Symposium on Cavitation*, edited by H. Murai (Sendai, Japan, 1986), pp. 67–72.